https://doi.org/10.17221/72/2026-PSE

Selenium promotes soybean sprout growth *via* enhanced antioxidant capacity and nutrient mobilisation

*Kaiwei Li[1,2], Lele Li[1,2], Yuqing Liu[1,2], Sanchun Lei[1,2], Minghao Hao[1,2], Qiong Wu[1,2], Feiyan Yu[1,2,3], Lianhe Zhang[1,2,3]**

[1]*Agricultural College, Henan University of Science and Technology, Luoyang City, Henan Province, P.R. China*
[2]*Luoyang Key Laboratory of Plant Nutrition and Environmental Ecology, Luoyang, Henan, P.R. China*
[3]*Henan Jinxiwang Agricultural Science and Technology Company Limited, Luoyang, Henan, P.R. China*
**Corresponding author: lhzhang2007@126.com*

Citation: Li K.W., Li L.L., Liu Y.Q., Lei S.C., Hao M.H., Wu Q., Yu F.Y., Zhang L.H. (2026): Selenium promotes soybean sprout growth *via* enhanced antioxidant capacity and nutrient mobilisation. Plant Soil Environ., 72: 284–297.

Abstract: Selenium (Se) biofortification of soybean sprouts presents a promising approach for enhancing dietary Se intake. However, the physiological mechanisms of Se promoting growth remain poorly understood. Here, we investigated the effects of selenite (Na_2SeO_3) at concentrations of 0, 2.5, 5.0, 7.5, and 10 μmol/L on soybean sprout development over 72 h. The results indicated that 5.0 and 7.5 μmol/L Na_2SeO_3 significantly promoted hypocotyl elongation and biomass accumulation. Se predominantly accumulated in the radicle, followed by the hypocotyl and cotyledon. Moderate selenite levels enhanced the activities of superoxide dismutase, peroxidase, and ascorbate peroxidase; increased the concentrations of reduced glutathione, ascorbic acid, and free proline; and effectively suppressed the accumulation of superoxide anion and hydrogen peroxide, thereby reducing malondialdehyde (MDA) concentration and alleviating oxidative stress. Concurrently, amylase and protease activities in cotyledons were stimulated, accelerating the hydrolysis of storage reserves. The resulting increases in soluble sugars, proteins, and free amino acids in the hypocotyl supported its elongation and biomass increase. In contrast, 10 μmol/L Na_2SeO_3 suppressed antioxidant enzyme activities, elevated reactive oxygen species and MDA levels, and inhibited growth. Collectively, these findings demonstrate that moderate Se enhances soybean sprout growth primarily by increasing antioxidant capacity, reducing oxidative stress, and facilitating the mobilisation of storage reserves toward the elongating hypocotyl, thereby revealing key physiological mechanisms for cultivating high-quality, Se-enriched sprouts.

Keywords: Se biofortification; antioxidant system; physiological characteristics; reserve mobilisation; growth promotion

Selenium (Se) is an essential trace element for human health, primarily through its incorporation into selenoproteins such as glutathione peroxidases (GPx), thioredoxin reductases (TrxR), and iodothyronine deiodinases (Labunskyy et al. 2014). These enzymes are crucial for antioxidant defence, thyroid hormone metabolism, and immune regulation, underpinning Se's roles in enhancing immunity, preventing inflammation, reducing cancer risk, and maintaining male fertility (White and Castellano 2016, Yang et al. 2025). Although the recommended daily intake for adults is 55 μg/day, Se deficiency affects over one billion

Supported by the National Natural Science Foundation of China-Henan Joint Fund, Project No. U1904114.

© The authors. This work is licensed under a Creative Commons Attribution 4.0 International Licence (CC BY 4.0).

https://doi.org/10.17221/72/2026-PSE

people globally (Jones et al. 2017). This public health concern is exacerbated in regions with low soil Se concentrations, including parts of China, Europe, and Africa, where it increases the risk of endemic diseases such as Keshan disease (a cardiomyopathy) and Kashin-Beck disease (an osteochondropathy) (Tan et al. 2002). Since dietary Se is predominantly derived from plant-based foods, increasing Se concentrations in agricultural products is a key strategy to improve human Se status.

Soybean (*Glycine max* L.) is a globally important oilseed crop. Its sprouts, produced by germinating seeds in the dark, are a traditional vegetable consumed year-round in Asia (Zhang et al. 2024) and valued for their crisp texture, rich nutrient profile, and affordability. They are abundant in health-promoting compounds, including soluble sugars, vitamin C (ascorbic acid), isoflavones, and phenolics. Vitamin C can scavenge reactive oxygen species (ROS) and prevent scurvy. Isoflavones contribute to hormone regulation, bone health, skin condition, mood modulation, and metabolism. During sprouting, storage proteins, carbohydrates, and fats in cotyledons are rapidly degraded into more bioavailable amino acids and soluble sugars (Bueno et al. 2020). Moreover, soybean sprouts efficiently convert absorbed inorganic Se into highly bioavailable organic forms, such as selenomethionine (SeMet) and selenocysteine (SeCys) (Huang et al. 2022), making them an ideal vegetable for Se biofortification. However, commercial production of soybean sprouts is often hampered by oxidative stress. Their vigorous growth and high metabolic rate can lead to excessive ROS accumulation, causing oxidative damage that manifests as radical decay, growth retardation, reduced yield, and poor quality.

Se, a beneficial element for plants, plays a dual role: optimal concentrations promote growth and enhance stress tolerance, while excess levels lead to toxicity (Ikram et al. 2024). At low doses, Se enhances the activities of antioxidant enzymes, including superoxide dismutase (SOD), peroxidase (POD), catalase (CAT), ascorbate peroxidase (APX), glutathione reductase (GR), and GPx, and also stimulates the synthesis of antioxidant metabolites. Consequently, Se improves ROS scavenging, maintains redox homeostasis, reduces membrane lipid peroxidation (Hasanuzzaman et al. 2020), and ultimately protects cellular integrity, supporting normal growth. For instance, Se application significantly increased antioxidant enzyme activities in tomato fruits (Godina et al. 2016) and enhanced the ascorbate-glutathione (AsA-GSH) cycle in germinating barley (Cheng et al. 2023). Furthermore, Se can increase the concentrations of free amino acids, sugars, and bioactive compounds such as phenolics and γ-aminobutyric acid (GABA) (Sun et al. 2024). Therefore, Se biofortification offers significant potential not only by alleviating oxidative stress and mitigating production challenges in soybean sprouts, but also by synergistically enhancing their nutritional quality to meet growing consumer demands.

Herein, we reveal the concentration-dependent physiological mechanism by which selenite enhances antioxidant capacity, mitigates oxidative stress, and promotes reserve mobilisation, thereby improving growth and Se enrichment in soybean sprouts. Our findings provide a mechanistic foundation for the production of high-quality, Se-enriched soybean sprouts and support the development of Se-enhanced functional vegetables.

MATERIAL AND METHODS

Plant material and experimental design. The soybean cv. Bayan was used in this study. Five hundred seeds with uniform size, intact appearance, and no visible damage were selected, surface-sterilised by washing and soaking in ozonated distilled water for 20 min, followed by immersion in distilled water for 10 min. Subsequently, seeds were soaked in distilled water in the dark for 12 h, then transferred to germination trays and incubated in distilled water in darkness at 30 °C for 24 h. Seeds with radicles approximately 1.5 cm in length were selected and transferred to germination boxes containing selenite solutions at concentrations of 0 (control), 2.5, 5.0, 7.5, and 10 μmol/L. All solutions contained 5 mmol/L calcium chloride ($CaCl_2$) to adjust osmotic potential. Fifty germinated seeds were placed in each box with their radicles immersed in the solution. The sprouts were cultivated in the dark at 30 °C for 72 h, and the selenite solutions were replaced every 24 h. After 72 h, samples were collected, immediately frozen in liquid nitrogen, and separated into radicle, hypocotyl, and cotyledon tissues. The length of the radicle and hypocotyl, as well as the fresh weight of each tissue, were measured. All samples were stored at –20 °C for subsequent physiological and biochemical analyses. All measurements were performed in triplicate.

Measurement of length. After treatment, ten uniformly grown sprouts from each group were selected.

https://doi.org/10.17221/72/2026-PSE

Radicle and hypocotyl lengths were measured using a ruler (0.01 cm precision).

Measurement of fresh weight. Fresh weights of radicle, hypocotyl, and cotyledon from ten representative soybean sprouts per treatment were measured using an analytical balance (0.001 g precision).

Determination of Se concentration. Se concentration was determined according to the method of Lei et al. (2025). The dried samples were weighed and digested with a 5 mL mixture of HNO_3:$HClO_4$ (4:1, *v*/*v*) overnight. Pre-digestion was performed at 100 °C for 60 min, followed by digestion at 150 °C for 240 min. After cooling, 2.5 mL of the acid mixture was added if necessary, and digestion continued at 150 °C for another 120 min. After cooling to below 50 °C, 2.5 mL of 6 mol/L HCl was added, and the mixture was heated at 100 °C for 180 min for reduction. The digest was cooled, transferred to a 25 mL volumetric flask, and diluted to volume with deionised water. Se concentration was measured by atomic fluorescence spectrometry (PF32, Beijing Purkinje General Instrument Co., Ltd., Beijing, China, 2017) using 5% HCl as carrier solution and a mixture of 1.5% KBH_4 and 0.5% NaOH as reductant. Operating parameters were as follows: carrier gas flow 300 mL/min, shield gas flow 600 mL/min, lamp current 40 mA, furnace height 25 mm, reading delay 7 s, and measurement time 22 s. Quantification was based on peak area integration.

Assay of SOD activity. SOD activity was assayed according to the method of Lei et al. (2025). A 0.2 g sample was homogenised in 1.8 mL of ice-cold 50 mmol/L phosphate buffer (pH 7.8). The homogenate was centrifuged at 10 000 rpm for 20 min at 4 °C, and the supernatant was collected. The reaction mixture (3 mL) contained 1.5 mL phosphate buffer (50 mmol/L, pH 7.8), 300 µL of 13 mmol/L methionine, 300 µL of 75 µmol/L nitro blue tetrazolium (NBT), 300 µL of 10 µmol/L EDTA-Na_2, 300 µL of 2 µmol/L riboflavin, 50 µL enzyme extract (or buffer instead of blank/control), and 250 µL distilled water. After mixing, tubes (except the blank, which was kept in the dark) were illuminated at 4 000 lx for 20 min. The reaction was stopped by covering the tubes with foil. Absorbance was measured at 560 nm using a spectrophotometer (Beijing Purkinje General Instrument Co., Ltd., Beijing, China, 2021), and the blank value was subtracted.

Assay of POD activity. POD activity was assayed according to the method of Lei et al. (2025). The enzyme extract was prepared as described for SOD. The reaction system contained 2.9 mL phosphate buffer (50 mmol/L, pH 5.5), 1 mL of 2% H_2O_2, 1 mL of 50 mmol/L guaiacol, and 0.1 mL enzyme extract. The control received heat-inactivated enzyme. After incubation at 37 °C for 15 min, the reaction was terminated by adding 2 mL of 20% trichloroacetic acid (TCA) and placing the tubes on ice. After centrifugation at 5 000 rpm for 10 min, absorbance of the supernatant was read at 470 nm.

Assay of APX activity. APX activity was assayed according to the method of Qi et al. (2023). Enzyme extraction followed the SOD method. The reaction mixture (3 mL) contained 0.1 mL enzyme extract, 2.6 mL phosphate buffer (50 mmol/L, pH 7.0, containing 0.1 mmol/L EDTA-Na_2), 0.15 mL of 5 mmol/L ascorbic acid, and 0.15 mL of 20 mmol/L H_2O_2 (added last to initiate reaction). The blank contained buffer instead of H_2O_2. Absorbance at 290 nm was recorded every 30 s for 3 min immediately after mixing.

Determination of GSH concentration. GSH concentration was determined according to the method of Lei et al. (2025). The supernatant obtained for SOD was used. To 250 µL extract, 2.6 mL of 150 mmol/L Na_2HPO_4 (pH 7.7) and 150 µL of DTNB (5,5'-dithiobis-2-nitrobenzoic acid) reagent were added. After mixing and incubation at 30 °C for 5 min, the absorbance was measured at 412 nm. The blank contained buffer instead of DTNB.

Determination of AsA concentration. AsA concentration was determined according to the method of Lei et al. (2025). Weigh approximately 0.2 g of fresh sample into a mortar, add 5 mL of 2% HCl, and grind to a homogenate. Transfer the homogenate to a 50 mL volumetric flask, rinse the mortar with small portions of 2% HCl, and dilute to the mark with the same solution. Mix well and filter. Collect 5 mL of the filtrate into a 10 mL volumetric flask, add 0.5 mL of 1% KI solution and 2.0 mL of 0.5% starch solution, then dilute to 10 mL with distilled water. Titrate the mixture with 0.001 mol/L KIO_3 solution until a faint blue colour persists for at least 30 s. Record the volume of KIO_3 consumed. Perform a blank titration using 5 mL of 2% HCl instead of the filtrate. Calculate the AsA concentration based on the titration difference.

Determination of free proline concentration. Free proline concentration was determined according to the method of Lei et al. (2025). A 0.2 g sample was extracted with 5 mL of 3% sulfosalicylic acid in boiling water for 10 min. After cooling and centrifugation, 2 mL of the supernatant was mixed with 2 mL glacial acetic acid and 3 mL 2.5% acid ninhydrin, heated

https://doi.org/10.17221/72/2026-PSE

in boiling water for 40 min, cooled, and extracted with 5 mL toluene. The toluene layer was measured at 520 nm.

Determination of superoxide anion (O_2^-) concentration. O_2^- concentration was determined according to the method of Qi et al. (2023). A 0.2 g sample was homogenised in 5 mL ice-cold phosphate buffer (50 mmol/L, pH 7.8) and centrifuged at 3 000 rpm for 10 min at 4 °C. The supernatant was centrifuged again at 12 000 rpm for 20 min. To 1 mL of the final supernatant, 0.5 mL phosphate buffer and 0.5 mL of 10 mmol/L hydroxylamine hydrochloride were added. After incubation at 25 °C for 30 min, 1 mL each of 17 mmol/L sulfanilamide and 7 mmol/L α-naphthylamine was added. After 15 min of colour development at 25 °C, absorbance was measured at 530 nm against a blank (water instead of the extract).

Determination of hydrogen peroxide (H_2O_2) concentration. H_2O_2 concentration was determined according to the method of Qi et al. (2023). A 0.2 g sample was homogenised in 2 mL of cold acetone. After centrifugation at 4 000 rpm for 10 min, 1 mL of the supernatant was mixed with 0.1 mL of 5% titanium sulfate and 0.2 mL of concentrated ammonia. The precipitate was collected by centrifugation (4 000 rpm, 10 min), washed five times with cold acetone, and then dissolved in 5 mL of 2 mol/L H_2SO_4. Absorbance was read at 415 nm.

Determination of malondialdehyde (MDA) concentration. MDA concentration was determined according to the method of Lei et al. (2025). The supernatant from the SOD extraction was used. A 300 µL aliquot of extract (or 5% TCA for control) was mixed with 300 µL of 0.6% thiobarbituric acid (TBA), heated in boiling water for 15 min, cooled, and centrifuged at 12 000 rpm for 1 min. Absorbance of the supernatant was measured at 532, 600, and 450 nm.

Assay of amylase activity. Amylase activity was assayed according to the method of Zeid et al. (2019). A 0.2 g sample was homogenised in 4 mL distilled water, adjusted to 10 mL, and centrifuged at 3 000 rpm for 10 min. The supernatant was diluted appropriately. For (α + β)-amylase, 1 mL diluted extract was mixed with 1 mL of 1% starch solution, incubated at 40 °C for 5 min, and the reaction was stopped with 2 mL of 3,5-dinitrosalicylic acid (DNS). For α-amylase alone, the extract was preheated at 70 °C for 15 min to inactivate β-amylase before the assay. After boiling for 5 min and dilution to 20 mL, the absorbance was measured at 540 nm.

Assay of protease activity. Protease activity was assayed according to the method of Zeid et al. (2019). A 0.2 g sample was homogenised in 5 mL borate buffer (pH 10.5), adjusted to 10 mL with the same buffer, and filtered. One millilitre of enzyme extract was mixed with 1 mL of 10 mg/mL casein (pre-warmed at 40 °C). After incubation at 40 °C for 10 min, 2 mL of 0.4 mol/L TCA was added. For the blank, TCA was added before casein. After standing for 10 min and filtration, 1 mL filtrate was mixed with 5 mL of 0.4 mol/L Na_2CO_3 and 1 mL Folin reagent, incubated at 40 °C for 20 min, and measured at 680 nm.

Determination of soluble sugar concentration. Soluble sugar concentration was determined according to the method of Lei et al. (2025). A 0.2 g sample was extracted with 15 mL of distilled water in boiling water for 20 min, cooled, filtered, and diluted to 100 mL. One millilitre of extract was mixed with 5 mL of anthrone reagent, boiled for 10 min, cooled, and measured at 620 nm.

Determination of soluble protein concentration. Soluble protein concentration was determined according to the method of Lei et al. (2025). The supernatant from the SOD extraction was used. A 20 µL aliquot was mixed with 1 mL phosphate buffer and 5 mL Coomassie Brilliant Blue G-250, incubated for 2 min, and measured at 595 nm against a blank (water instead of extract).

Determination of free amino acid concentration. Free amino acid concentration was determined according to the method of Lei et al. (2025). A 0.2 g sample was homogenised in 5 mL of 10% acetic acid, diluted to 100 mL, and filtered. One millilitre of filtrate was mixed with 1 mL of water, 3 mL of ninhydrin reagent, and 0.1 mL of 0.1% ascorbic acid, heated in boiling water for 15 min, cooled, diluted to 20 mL with 60% ethanol, and measured at 570 nm.

Statistical analysis. All data are presented as mean ± standard deviation (SD) of three independent replicates. Statistical analysis was performed using SPSS 26.0 (SPSS Inc., Chicago, USA). One-way ANOVA with Duncan's test was used to determine significant differences among treatments at $P < 0.05$. Graphs were generated using GraphPad Prism 10.1.2 (GraphPad Software, LLC, San Diego, USA).

RESULTS

Effects of selenite treatments on the growth of soybean sprouts. The growth of soybean sprouts exhibited a marked concentration-dependent re-

https://doi.org/10.17221/72/2026-PSE

Table 1. Effects of selenite concentrations on radicle length, hypocotyl length, and biomass of various tissues in soybean sprouts

Selenite solution levels (μmol/L)	Radicle	Hypocotyl	Radicle	Hypocotyl	Cotyledon
	length (cm)		fresh weight (g)		
0	5.46 ± 0.27^{c}	7.84 ± 0.22^{cd}	0.042 ± 0.002^{d}	0.21 ± 0.00^{bc}	0.28 ± 0.00^{ab}
2.5	6.19 ± 0.13^{b}	8.36 ± 0.14^{bc}	0.048 ± 0.001^{c}	0.22 ± 0.00^{b}	0.27 ± 0.00^{b}
5.0	6.53 ± 0.18^{ab}	8.64 ± 0.18^{b}	0.053 ± 0.001^{b}	0.24 ± 0.00^{a}	0.26 ± 0.00^{c}
7.5	6.88 ± 0.18^{a}	9.33 ± 0.21^{a}	0.059 ± 0.001^{a}	0.25 ± 0.00^{a}	0.25 ± 0.01^{c}
10	5.19 ± 0.22^{c}	7.53 ± 0.26^{d}	0.039 ± 0.001^{d}	0.21 ± 0.01^{c}	0.29 ± 0.01^{a}

The radicles of soybean sprouts were cultured in selenite solutions at concentrations of 0, 2.5, 5.0, 7.5, and 10 μmol/L for 3 days. Radicle length, hypocotyl length, and fresh weight of each tissue were measured upon sampling. Data are presented as mean ± SD (n = 3). Different lowercase letters within the same column indicate significant differences among treatments at $P < 0.05$ (Duncan's test)

sponse to selenite treatments (Table 1). Selenite at concentrations of 5.0 and 7.5 μmol/L significantly promoted elongation and fresh weight accumulation in the radicle and hypocotyl, while reducing cotyledon fresh weight. Specifically, compared to the control, radicle length increased significantly by 13.4, 19.6, and 26.0% at 2.5, 5.0, and 7.5 μmol/L Na_2SeO_3, respectively, while its fresh weight increased significantly by 14.8, 27.1, and 40.7%, respectively. Hypocotyl length was significantly enhanced by 10.2% and 19.0% at 5.0 and 7.5 μmol/L, respectively, and its fresh weight increased significantly by 16.1% and 19.0%. In contrast, cotyledon fresh weight decreased significantly by 9.0% and 11.9% at the same concentrations. However, at 10 μmol/L, these promotive effects were abolished. Radicle length showed no difference from the control, while hypocotyl length decreased by 4.0%, but no significant difference was observed. Radicle fresh weight remained comparable to the control; hypocotyl decreased slightly, and cotyledon showed a marginal recovery, though none of these differences was statistically significant.

Effects of selenite treatments on Se accumulation in soybean sprouts. Selenite treatments at concentrations ranging from 0 to 10 μmol/L resulted in a significant, concentration-dependent increase in Se accumulation across all examined soybean sprout tissues ($P < 0.05$). As shown in Table 2, the radicle exhibited the highest Se enrichment, followed by the hypocotyl and then the cotyledon. Significant differences in Se concentration were observed both among treatments within the same tissue and among different tissues at the same treatment level, indicating that Se uptake and translocation in soybean sprouts are tissue-specific.

Effects of selenite treatments on antioxidant enzyme activities in soybean sprouts. SOD, POD, and APX are key antioxidant enzymes that play vital roles in scavenging ROS and mitigating oxidative damage. As shown in Figure 1, selenite treatment significantly

Table 2. Effects of selenite solution levels on selenium (Se) concentrations in the radicle, hypocotyl, and cotyledon of soybean sprouts

Selenite solution levels (μmol/L)	Radicle	Hypocotyl	Cotyledon
	Se concentration (mg/kg DW)		
0	5.35 ± 0.83^{e}	0.19 ± 0.02^{e}	0.05 ± 0.00^{e}
2.5	29.29 ± 1.18^{d}	2.85 ± 0.25^{d}	0.44 ± 0.01^{d}
5.0	49.42 ± 2.55^{c}	6.81 ± 0.35^{c}	0.91 ± 0.02^{c}
7.5	64.93 ± 1.81^{b}	9.10 ± 0.11^{b}	1.47 ± 0.02^{b}
10	94.26 ± 4.85^{a}	16.10 ± 2.04^{a}	3.04 ± 0.12^{a}

The radicles of soybean sprouts were cultured in selenite solutions at concentrations of 0, 2.5, 5.0, 7.5, and 10 μmol/L for 3 days. Data are presented as mean ± SD (n = 3). Different lowercase letters within the same column indicate significant differences among treatments at $P < 0.05$ (Duncan's test). DW – dried weight

https://doi.org/10.17221/72/2026-PSE

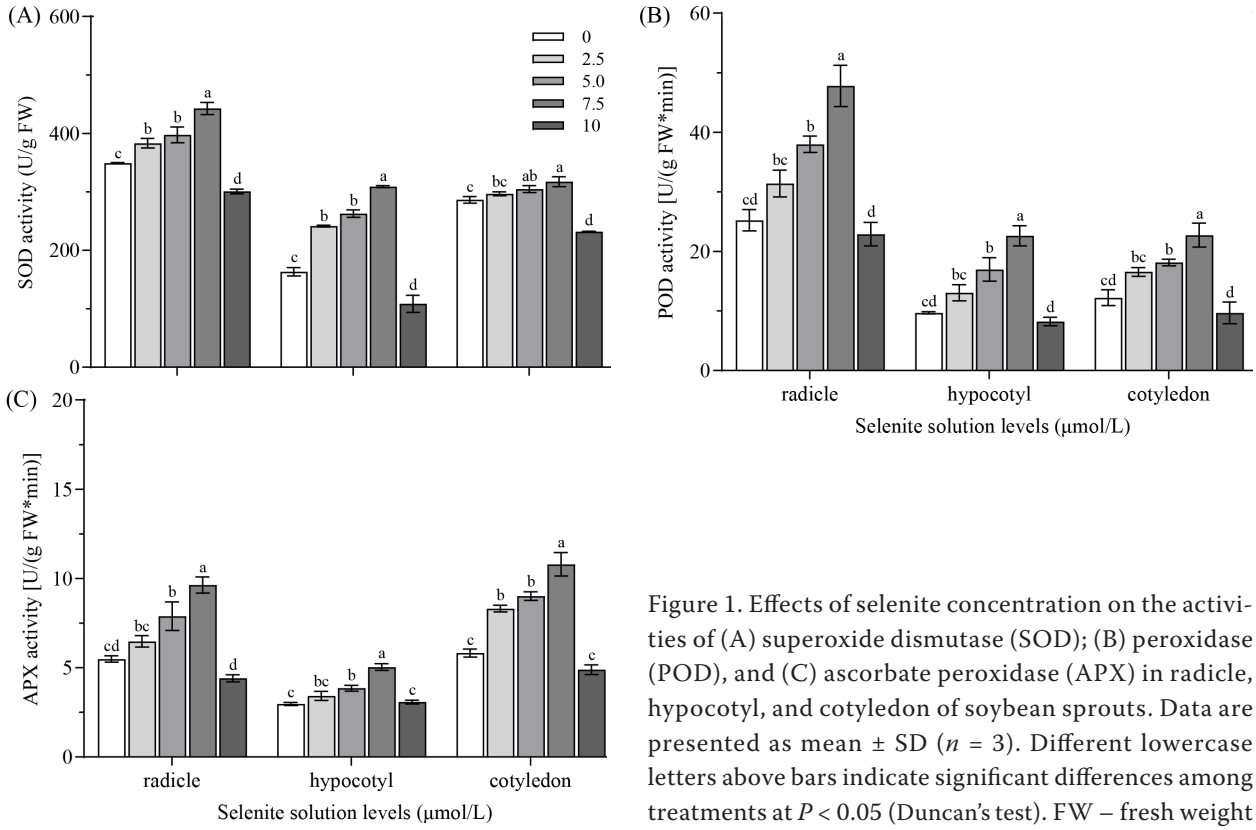

Figure 1. Effects of selenite concentration on the activities of (A) superoxide dismutase (SOD); (B) peroxidase (POD), and (C) ascorbate peroxidase (APX) in radicle, hypocotyl, and cotyledon of soybean sprouts. Data are presented as mean ± SD (n = 3). Different lowercase letters above bars indicate significant differences among treatments at $P < 0.05$ (Duncan's test). FW – fresh weight

influenced the activities of these enzymes in a concentration-dependent manner across all examined tissues of soybean sprouts. In the radicle, SOD activity increased significantly by 9.7, 13.8, and 26.7% at 2.5, 5.0, and 7.5 μmol/L Na_2SeO_3, respectively. The hypocotyl exhibited a more pronounced rise, with increases of 47.9, 61.1, and 89.2% at the same concentrations. In the cotyledon, SOD activity was significantly elevated only at 5.0 and 7.5 μmol/L, with increases of 6.5% and 10.9%, respectively. However, treatment with 10 μmol/L Na_2SeO_3 significantly suppressed SOD activity across all tissues, reducing it by 13.9, 33.5, and 18.9% in the radicle, hypocotyl, and cotyledon, respectively (Figure 1A). At 5.0 and 7.5 μmol/L Na_2SeO_3, POD activity increased significantly. In the radicle, the increases were 50.5% and 89.4%, respectively; in the hypocotyl, the increases were even greater, reaching 75.1% and 133.6%; and in the cotyledon, the increases were 48.2% and 85.6%, respectively. In contrast, the 10 μmol/L treatment induced a slight decline in POD activity across all tissues compared with the control (Figure 1B). In the radicle, APX activity increased significantly by 43.8% and 75.7% at 5.0 and 7.5 μmol/L, respectively. The hypocotyl showed significant increases of 29.9% and 69.6% at the same concentrations. In the cotyledon, APX activity was significantly elevated even at 2.5 μmol/L Na_2SeO_3, with increases of 42.9, 54.9, and 85.5% at 2.5, 5.0, and 7.5 μmol/L, respectively. At 10 μmol/L, APX activity showed a non-significant declining trend in the radicle, with no differences observed in the hypocotyl or cotyledon (Figure 1C).

Effects of selenite treatments on non-enzymatic antioxidant concentration in soybean sprouts. GSH, AsA, and proline are key non-enzymatic antioxidants that scavenge ROS and maintain redox homeostasis, while proline also serves as a major osmolyte, helping plants regulate osmotic pressure under stress conditions. As shown in Figure 2, selenite treatment significantly influenced the concentrations of GSH, AsA, and free proline in a concentration-dependent manner across various tissues of soybean sprouts, exhibiting a concentration-dependent pattern, with free proline accumulation also exhibiting tissue specificity. At 2.5, 5.0, and 7.5 μmol/L Na_2SeO_3, GSH concentration in the radicle increased significantly by 17.7, 22.5, and 40.1%, respectively. The cotyledon showed a more pronounced accumulation, with increases of 23.3, 36.0, and 70.2% at the same concentrations. In the hypocotyl, GSH concentration rose significantly by 24.4% and 28.8% at 5.0 and 7.5 μmol/L, respectively. At 10 μmol/L, GSH declined significantly compared with the 7.5 μmol/L treatment but remained slightly

https://doi.org/10.17221/72/2026-PSE

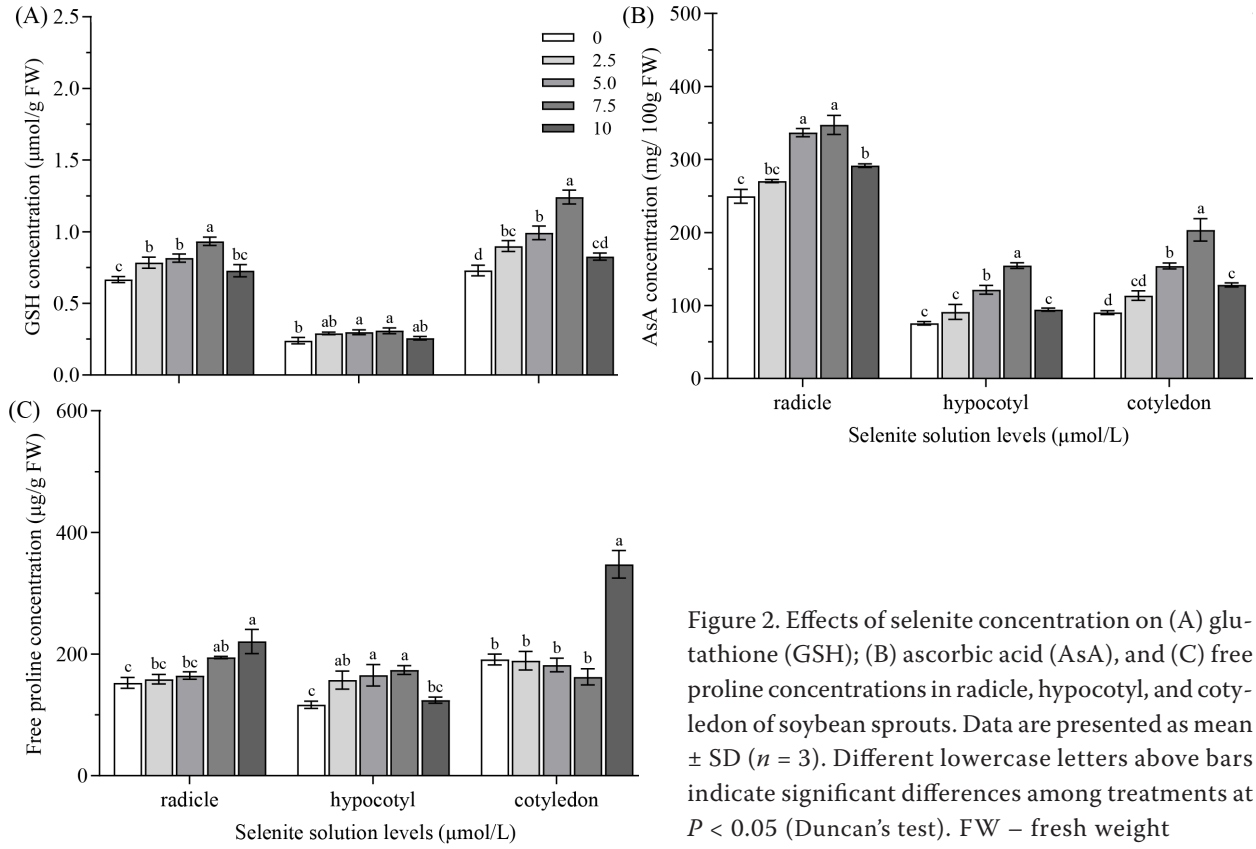

Figure 2. Effects of selenite concentration on (A) glutathione (GSH); (B) ascorbic acid (AsA), and (C) free proline concentrations in radicle, hypocotyl, and cotyledon of soybean sprouts. Data are presented as mean ± SD (n = 3). Different lowercase letters above bars indicate significant differences among treatments at $P < 0.05$ (Duncan's test). FW – fresh weight

higher than the control in all tissues (Figure 2A). At 5.0 and 7.5 μmol/L Na_2SeO_3, AsA concentration in the radicle increased significantly by 34.9% and 39.2%, respectively, while hypocotyl significantly rose by 60.7% and 104.5%. In the cotyledon, AsA concentration showed the greatest enhancement at the same concentrations, increasing by 70.6% and 125.2%, respectively. At 10 μmol/L, AsA declined significantly in all tissues relative to the 7.5 μmol/L treatment. Nevertheless, AsA levels in the radicle and cotyledon remained significantly higher than the control, with increases of 16.8% and 42.0%, respectively, while hypocotyl showed no difference (Figure 2B). Free proline concentration in the radicle increased significantly by 27.4% and 44.7% at 7.5 and 10 μmol/L Na_2SeO_3, respectively. In the hypocotyl, proline concentration significantly rose by 34.8, 41.6, and 48.9% at 2.5, 5.0, and 7.5 μmol/L, respectively; at 10 μmol/L, it was higher than the control but not significantly different. In the cotyledon, free proline concentration increased markedly only at 10 μmol/L, with a rise of 81.8% (Figure 2C).

Effects of selenite treatments on ROS concentrations in soybean sprouts. O_2^- and H_2O_2 are reactive oxygen species capable of inducing oxidative stress and causing oxidative damage to cell membranes. As shown in Figure 3, selenite treatment exerted a significant dual regulatory effect on O_2^- and H_2O_2 concentrations across all examined tissues of soybean sprouts. At 2.5, 5.0, and 7.5 μmol/L Na_2SeO_3, O_2^- concentration decreased significantly by 14.3, 18.0, and 25.6% in the radicle, respectively, and by 14.1, 18.6, and 30.1% in the hypocotyl. In the cotyledon, O_2^- concentration significantly declined by 22.5% and 33.3% at 5.0 and 7.5 μmol/L, respectively. However, at 10 μmol/L, O_2^- concentration in all tissues increased significantly and exceeded the control levels, with increases of 12.6, 13.2, and 9.5% in the radicle, hypocotyl, and cotyledon, respectively (Figure 3A). At 5.0 and 7.5 μmol/L Na_2SeO_3, H_2O_2 concentration in the radicle decreased significantly by 6.9% and 11.3%, respectively, while that in the hypocotyl was significantly reduced by 9.7% and 13.2%. In the cotyledon, H_2O_2 concentration declined significantly by 8.9, 13.6, and 17.8% at 2.5, 5.0, and 7.5 μmol/L, respectively. However, at 10 μmol/L, H_2O_2 concentration increased significantly by 7.3, 11.1, and 8.4% in the radicle, hypocotyl, and cotyledon, respectively (Figure 3B).

Effects of selenite concentration on MDA concentration in soybean sprouts. MDA, a terminal

https://doi.org/10.17221/72/2026-PSE

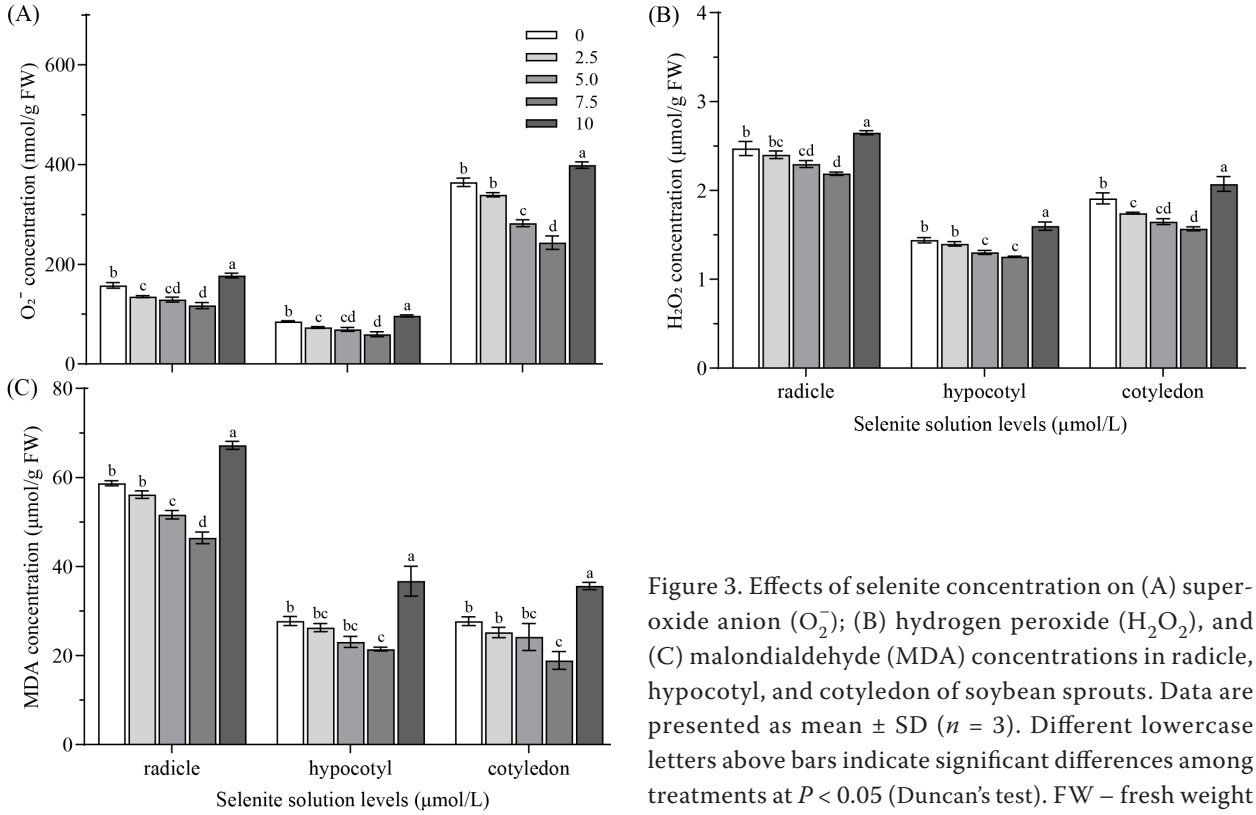

Figure 3. Effects of selenite concentration on (A) superoxide anion (O_2^-); (B) hydrogen peroxide (H_2O_2), and (C) malondialdehyde (MDA) concentrations in radicle, hypocotyl, and cotyledon of soybean sprouts. Data are presented as mean ± SD (n = 3). Different lowercase letters above bars indicate significant differences among treatments at $P < 0.05$ (Duncan's test). FW – fresh weight

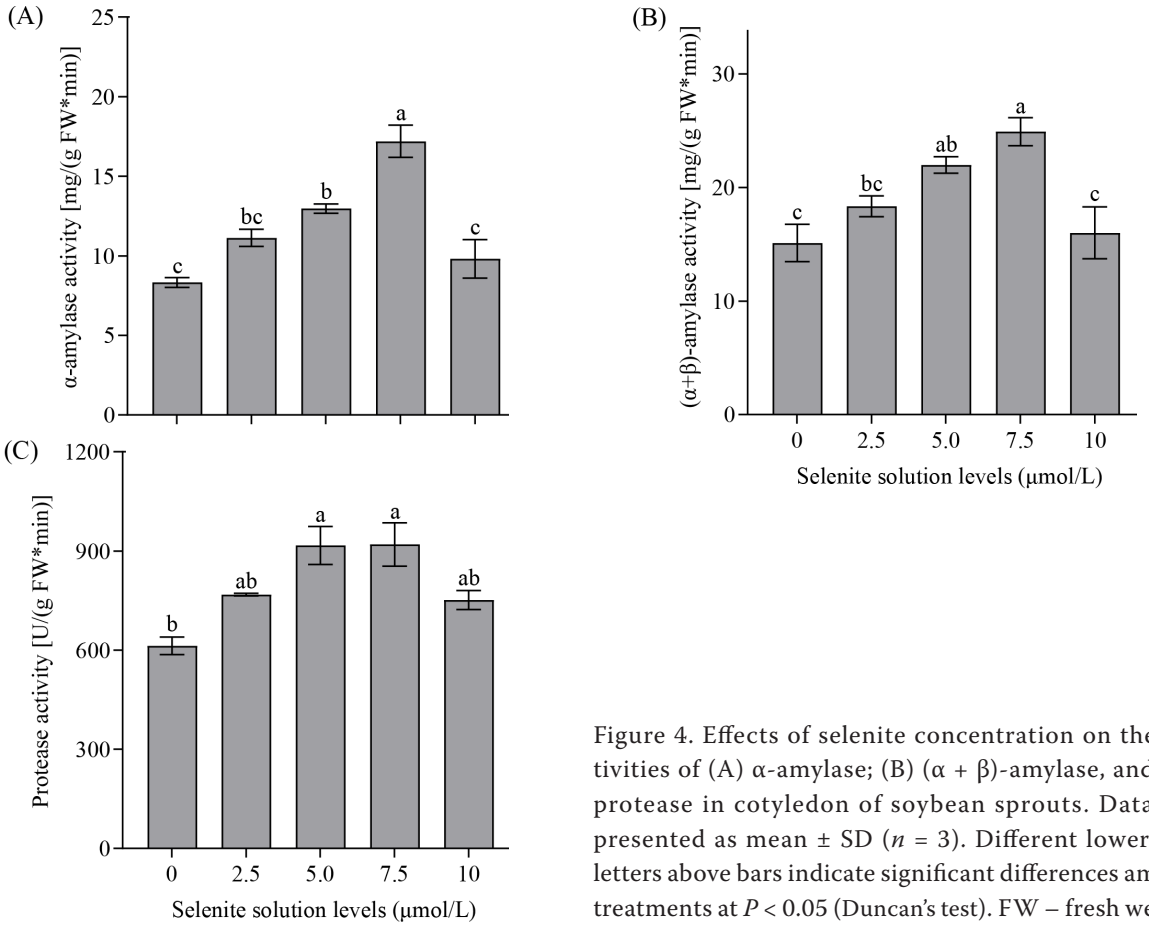

Figure 4. Effects of selenite concentration on the activities of (A) α-amylase; (B) (α + β)-amylase, and (C) protease in cotyledon of soybean sprouts. Data are presented as mean ± SD (n = 3). Different lowercase letters above bars indicate significant differences among treatments at $P < 0.05$ (Duncan's test). FW – fresh weight

https://doi.org/10.17221/72/2026-PSE

product of membrane lipid peroxidation, directly reflects the extent of oxidative damage to cellular membranes. As shown in Figure 3C, selenite treatment exerted a significant concentration-dependent effect on MDA accumulation across all examined tissues of soybean sprouts. At 5.0 and 7.5 μmol/L Na_2SeO_3, MDA concentration in the radicle decreased significantly by 12.0% and 20.9%, respectively. At 7.5 μmol/L, MDA concentration was significantly reduced by 22.7% in the hypocotyl and 31.8% in the cotyledon. However, at 10 μmol/L, MDA concentration increased significantly by 14.5, 32.3, and 28.6% in the radicle, hypocotyl, and cotyledon, respectively.

Effects of selenite concentration on amylase activity in soybean sprout cotyledons. Amylases catalyse the hydrolysis of starch into soluble sugars, a process essential for energy supply during germination. α-amylase cleaves internal α-1,4-glycosidic bonds randomly within starch chains, whereas β-amylase sequentially releases maltose units from the non-reducing ends. As shown in Figure 4A-B, selenite treatment significantly affected the activities of both α-amylase and (α + β)-amylase in the cotyledon of soybean sprouts. They exhibited a similar concentration-dependent pattern characterised by an initial increase followed by a decline. At 7.5 μmol/L Na_2SeO_3, α-amylase activity reached its peak, being significantly elevated by 106.4% compared to the control. A significant rise of 55.7% was also observed at 5.0 μmol/L. In contrast, at 2.5 and 10 μmol/L Na_2SeO_3, α-amylase activity did not differ significantly from the control. Similarly, (α + β)-amylase activity was significantly enhanced by 64.8% at 7.5 μmol/L and by 45.4% at 5.0 μmol/L Na_2SeO_3. No significant differences were detected at 2.5 and 10 μmol/L Na_2SeO_3 compared to the control.

Effects of selenite concentration on protease activity in soybean sprout cotyledons. Proteases hydrolyse peptide bonds, facilitating protein degradation and reutilisation, and play a key role in regulating plant growth and adapting to nutrient demands. As shown in Figure 4C, selenite treatment exerted a concentration-dependent modulation on protease activity in the cotyledon of soybean sprouts. Protease activity initially increased, then declined with increasing selenite concentration, peaking at 5.0 and 7.5 μmol/L Na_2SeO_3, where it was significantly elevated by 49.5% and 50.0%, respectively, compared to the control. No significant difference in protease activity was observed between the 2.5

Table 3. Effects of selenite concentration on soluble sugar, soluble protein and free amino acid concentrations of various tissues in soybean sprouts

	Selenite solution levels (μmol/L)	Radicle	Hypocotyl	Cotyledon
Soluble sugar (mg/g FW)	0	16.43 ± 0.63^{c}	16.73 ± 0.27^{cd}	8.70 ± 0.54^{c}
	2.5	18.65 ± 0.97^{c}	19.00 ± 0.94^{c}	11.31 ± 0.77^{c}
	5.0	21.71 ± 0.60^{b}	22.89 ± 0.59^{b}	14.55 ± 0.49^{b}
	7.5	23.10 ± 0.94^{b}	27.67 ± 1.26^{a}	17.93 ± 1.04^{a}
	10	26.48 ± 0.84^{a}	15.32 ± 0.40^{d}	9.92 ± 0.96^{c}
Soluble protein (mg/g FW)	0	36.45 ± 2.04^{c}	21.78 ± 0.45^{bc}	79.66 ± 1.85^{a}
	2.5	38.47 ± 0.74^{c}	22.07 ± 0.39^{bc}	70.28 ± 2.62^{bc}
	5.0	42.99 ± 0.61^{b}	25.04 ± 1.52^{ab}	67.78 ± 0.27^{bc}
	7.5	46.90 ± 1.07^{b}	27.30 ± 1.23^{a}	63.94 ± 2.61^{c}
	10	54.90 ± 1.08^{a}	20.67 ± 0.95^{c}	74.28 ± 3.51^{ab}
Free amino acid (mg/g FW)	0	12.28 ± 1.99^{d}	16.96 ± 3.07^{c}	14.80 ± 1.46^{c}
	2.5	35.88 ± 0.97^{c}	55.52 ± 8.91^{b}	65.65 ± 8.70^{b}
	5.0	46.20 ± 4.67^{bc}	93.19 ± 2.08^{a}	81.02 ± 7.40^{b}
	7.5	59.70 ± 4.33^{b}	92.03 ± 4.74^{a}	122.10 ± 3.04^{a}
	10	80.87 ± 4.74^{a}	19.11 ± 2.32^{c}	27.58 ± 2.63^{c}

The radicles of soybean sprouts were cultured in selenite solutions at concentrations of 0, 2.5, 5.0, 7.5, and 10 μmol/L for 3 days. Data are presented as mean ± SD (n = 3). Different lowercase letters within the same column indicate significant differences among treatments at $P < 0.05$ (Duncan's test). FW – fresh weight

https://doi.org/10.17221/72/2026-PSE

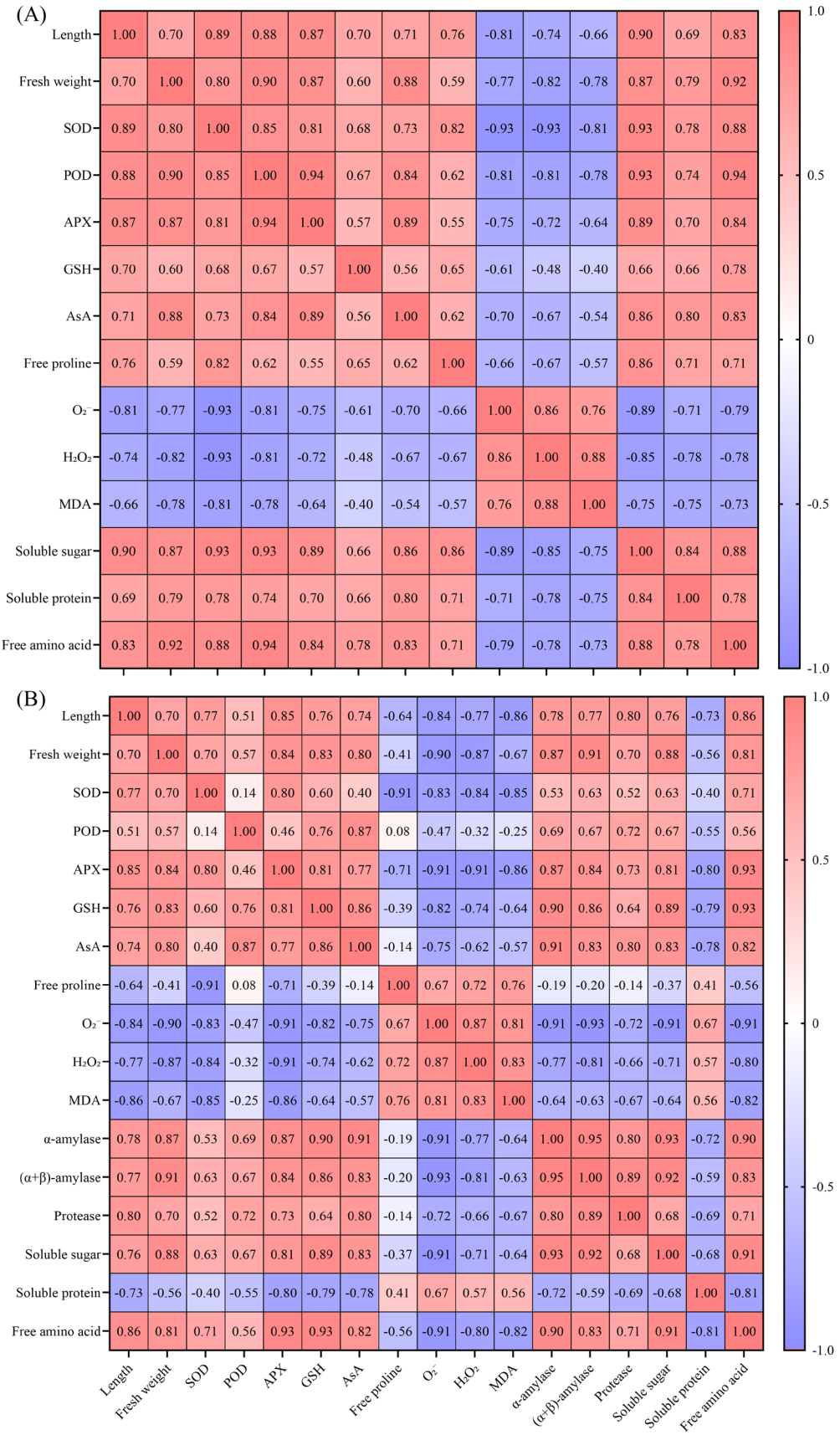

Figure 5. Correlation analysis between growth parameters of soybean sprouts with various physiological and biochemical indicators in the hypocotyl and cotyledons. The indicators shown in the figure are: length and fresh weight of hypocotyl, activities of superoxide dismutase (SOD), peroxidase (POD), ascorbate peroxidase (APX), concentrations of glutathione (GSH), ascorbic acid (AsA), free proline, superoxide anion (O_2^-), hydrogen peroxide (H_2O_2), malondialdehyde (MDA), soluble sugar, soluble protein, and free amino acid in the hypocotyl (A) and cotyledon (B), as well as activities of α-amylase, (α + β)-amylase, and protease in the cotyledon (B)

https://doi.org/10.17221/72/2026-PSE

and 10 μmol/L Na_2SeO_3. Although both were higher than the control, neither increase was significant.

Effects of selenite concentration on the quality of soybean sprouts. The results presented in Table 3 demonstrate that selenite treatment significantly alters the composition of key metabolites associated with soybean sprout nutritional quality. The effects were concentration- and tissue-dependent: low to moderate concentrations (2.5–7.5 μmol/L) generally increased metabolite levels, whereas the highest concentration (10 μmol/L) suppressed them in certain tissues. Soluble sugars serve as essential energy sources and participate in osmoregulation and respiration. At 5.0, 7.5, and 10 μmol/L Na_2SeO_3, soluble sugar concentration in the radicle increased significantly by 32.1, 40.6, and 61.1%, respectively. At 5.0 and 7.5 μmol/L, soluble sugar concentration increased significantly by 36.8% and 65.4% in the hypocotyl, respectively, and by 67.2% and 106.1% in the cotyledon. Soluble proteins play vital roles in maintaining cellular structure, function, and development. In the radicle, soluble protein concentration increased significantly by 17.9, 28.7, and 50.6% at 5.0, 7.5, and 10 μmol/L Na_2SeO_3, respectively. In the hypocotyl, a significant 25.3% increase was observed only at 7.5 μmol/L. Conversely, soluble protein concentration in the cotyledon decreased significantly by 11.8, 14.9, and 19.7% at 2.5, 5.0, and 7.5 μmol/L, respectively, suggesting degradation of storage proteins to support growth demands. Free amino acids, important products of nitrogen metabolism, are involved in growth promotion and stress responses. In the radicle, free amino acid concentration increased significantly in a concentration-dependent manner, showing 1.92-, 2.76-, 3.86-, and 5.59-fold increases at 2.5, 5.0, 7.5, and 10 μmol/L Na_2SeO_3, respectively. At 2.5, 5.0, and 7.5 μmol/L, free amino acid concentration increased significantly by 2.27-, 4.50-, and 4.43-fold in the hypocotyl, respectively, and by 3.44-, 4.47-, and 7.25-fold in the cotyledon. At 10 μmol/L Na_2SeO_3, soluble sugar, soluble protein, and free amino acid concentrations in the hypocotyl and cotyledon declined significantly compared with the 7.5 μmol/L treatment and returned to control levels, indicating that excessive selenite suppresses nutritional quality in these tissues.

Correlations of antioxidant enzymes, non-enzymatic antioxidants, and nutrient mobilisation indicators with growth parameters in Se-treated soybean sprouts. Under exogenous Se application, Pearson correlation analysis (Figure 5) was performed to evaluate the relationships between hypocotyl length, fresh weight, and various physiological indicators in soybean sprouts. As shown in Figure 5A, for hypocotyl length, highly significant positive correlations ($P < 0.01$) were observed with SOD, POD, APX, GSH, AsA, free proline, soluble sugar, soluble protein, and free amino acids, whereas O_2^-, H_2O_2, and MDA showed highly significant negative correlations ($P < 0.01$). Regarding fresh weight, SOD, POD, APX, AsA, soluble sugar, soluble protein, and free amino acids were highly significantly positively correlated ($P < 0.01$), while GSH and free proline exhibited significant positive correlations ($P < 0.05$); O_2^-, H_2O_2, and MDA were highly significantly negatively correlated ($P < 0.01$). As shown in Figure 5B, hypocotyl length was highly significantly positively correlated ($P < 0.01$) with SOD, APX, GSH, AsA, α-amylase, (α + β)-amylase, protease, soluble sugar, and free amino acids in cotyledon, and highly significantly negatively correlated ($P < 0.01$) with O_2^-, H_2O_2, MDA, and soluble protein, while free proline showed a significant negative correlation ($P < 0.05$). For hypocotyl fresh weight, highly significant positive correlations ($P < 0.01$) were found with SOD, APX, GSH, AsA, α-amylase, (α + β)-amylase, soluble sugar, and free amino acids; POD and protease showed significant positive correlations ($P < 0.05$). In contrast, O_2^-, H_2O_2, and MDA were highly significantly negatively correlated ($P < 0.01$), and soluble protein exhibited a significant negative correlation ($P < 0.05$). Collectively, promoting hypocotyl elongation and fresh weight accumulation in soybean sprouts can be achieved by enhancing the activities of antioxidant enzymes (SOD, POD, APX) and increasing the concentrations of non-enzymatic antioxidants (GSH, AsA) in hypocotyl, enhancing amylase and protease activities of cotyledon, accumulating soluble sugars and free amino acids in hypocotyl, while simultaneously reducing ROS (O_2^-, H_2O_2).

DISCUSSION

This study elucidates the physiological mechanisms underlying Se-induced growth promotion in soybean sprouts (Figure 6). Moderate Se supplementation (5.0–7.5 μmol/L) enhances hypocotyl elongation and biomass accumulation through a coordinated hormetic response. This growth stimulation is primarily mediated by Se's role as a redox modulator: optimal concentrations fortify both enzymatic (SOD, POD, and APX) and non-enzymatic (GSH, AsA, and free

https://doi.org/10.17221/72/2026-PSE

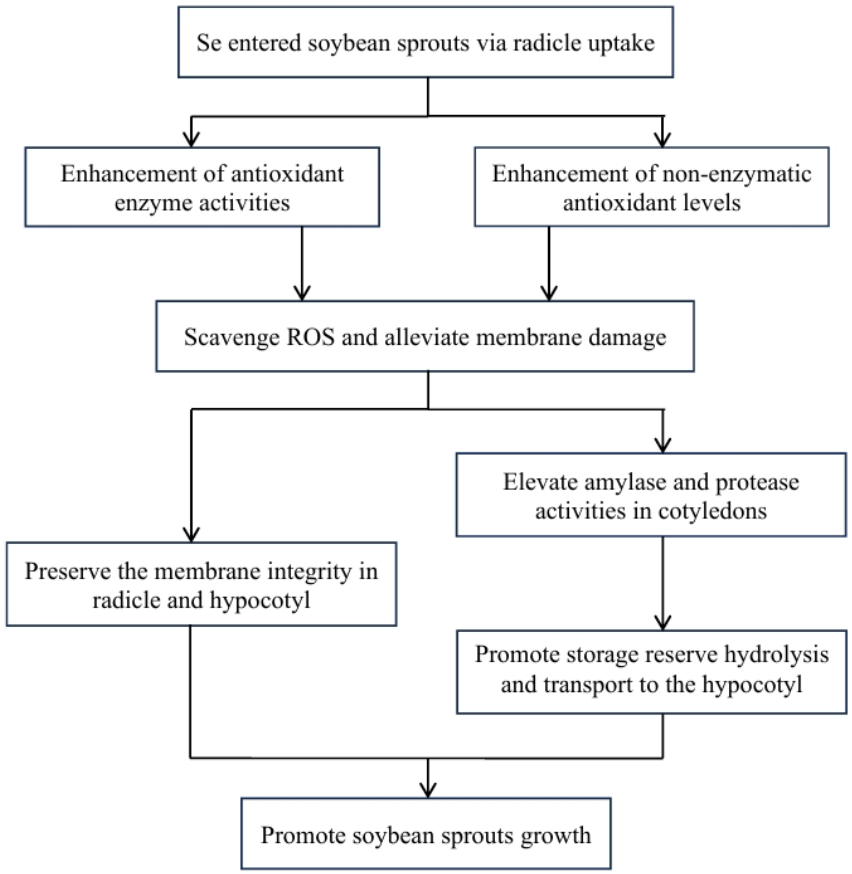

Figure 6. Physiological mechanisms underlying selenium (Se)-promoted growth of soybean sprouts. ROS – reactive oxygen species

proline) antioxidant networks, thereby maintaining cellular redox homeostasis. The consequent suppression of ROS accumulation and lipid peroxidation preserves membrane integrity and protects hydrolytic enzymes in cotyledons from oxidative inactivation. This enables accelerated mobilisation of storage reserves, which are translocated to the growing radicle and hypocotyl to fuel cell expansion and biomass synthesis. Conversely, 10 μmol/L Na_2SeO_3 exceeds the physiological threshold, disrupting redox balance, inducing oxidative damage, and impairing reserve mobilisation, ultimately inhibiting growth.

The observed tissue-specific Se gradient (radicle > hypocotyl > cotyledon) reflects constrained systemic translocation under dark germination (Table 2). Upon uptake, selenite is rapidly assimilated into organic forms (e.g., SeMet) and incorporated into root proteins (Li et al. 2008, Zhang et al. 2019), effectively sequestering Se in the radicle and limiting its mobility in free form (Mangiapane et al. 2014). Long-distance transport to shoots relies primarily on xylem-driven mass flow; however, the absence of transpirational pull in dark-grown sprouts restricts upward flux, allowing only minimal Se delivery *via* root pressure. Concurrently, the cotyledon functions as a transient source, rapidly hydrolysing reserves and exporting solutes toward sink tissues. Any SeMet reaching the cotyledon is likely remobilised downward to support the elongating radicle, while the hypocotyl acts predominantly as a conductive pathway. Together, limited xylem transport, active root assimilation, and source-to-sink remobilisation establish the observed distribution pattern.

Se modulates the antioxidant defence system in a strictly concentration-dependent manner. At 5.0–7.5 μmol/L Na_2SeO_3, coordinated upregulation of SOD, POD, and APX activities establishes an efficient ROS-scavenging cascade, while elevated GSH, AsA, and free proline provide substantial reducing capacity and osmoprotection (Figures 1–2). This reinforced network significantly suppresses O_2^- and H_2O_2 accumulation, minimising membrane lipid peroxidation and preserving cellular function across all tissues, thereby promoting the growth of soybean sprouts (Figure 3, Table 1). The correlation analysis (Figure 5A) further substantiates these relationships: in hypocotyl datasets, the positive associations of SOD, POD, APX, and AsA with growth parameters were highly

https://doi.org/10.17221/72/2026-PSE

significant ($P < 0.01$), while O_2^-, H_2O_2, and MDA exhibited consistently negative correlations ($P < 0.01$). At 10 μmol/L, however, excessive Se incorporation disrupts sulfur metabolism, leading to misfolded proteins and compromised antioxidant enzyme function (Van Hoewyk 2013, Gupta and Gupta 2017). The resulting ROS burst and MDA surge trigger a defensive osmolyte response, manifested as excessive accumulation of free proline, free amino acids, soluble sugars, and soluble proteins in the radicle (Figures 2C and 3, Table 3). However, this compensatory mechanism is insufficient to prevent oxidative damage and growth inhibition.

Under dark cultivation, soybean sprouts rely entirely on cotyledonary reserves, as photosynthetic carbon fixation and external nitrogen uptake are absent. Optimal Se concentrations significantly enhance amylase and protease activities in cotyledons (Malik et al. 2011, Zhou et al. 2024), accelerating starch and protein hydrolysis into soluble sugars and free amino acids (Figure 4, Table 3). These metabolites are efficiently exported *via* the hypocotyl to support radicle and hypocotyl development (Table 1). Correlation analysis (Figure 5B) strongly supports this source-to-sink model: hypocotyl length and fresh weight were highly significantly positively correlated ($P < 0.01$) with α-amylase, (α + β)-amylase, soluble sugar, and free amino acids in cotyledons, while soluble protein exhibited a significant negative correlation ($P < 0.05$). These findings indicate that enhanced hydrolytic enzyme activities and the accumulation of mobilised metabolites (sugars and amino acids), rather than the storage proteins themselves, are closely linked to improved growth. At 7.5 μmol/L Na_2SeO_3, the enrichment of soluble nutrients (sugars, proteins, and amino acids) and the peak accumulation of AsA substantially enhance the nutritional and functional quality of the edible hypocotyl (Table 3, Figure 2B). This source-to-sink redistribution underscores Se's dual role in promoting both physiological growth and nutritional biofortification.

Collectively, our findings demonstrate that moderate Se supplementation enhances soybean sprout development by reinforcing antioxidant capacity, mitigating oxidative stress, and optimising source-to-sink partitioning of cotyledonary reserves. This mechanistic framework establishes a physiological basis for precise Se dosing in soybean sprout biofortification protocols. Future studies should delineate the transcriptional and post-translational regulation of antioxidant and hydrolytic enzyme networks by Se, enabling targeted metabolic engineering and optimised cultivation strategies for high-quality, Se-enriched functional foods.

Acknowledgement. We thank the Experimental Teaching Centre of the Agricultural University for its strong support for the experiment. This study was financially supported by the National Natural Science Foundation of China-Henan Joint Fund, Project No. U1904114.

REFERENCES

Bueno D.B., Da Silva Júnior S.I., Seriani Chiarotto A.B., Cardoso T.M., Neto J.A., Lopes Dos Reis G.C., Glória M.B.A., Tavano O.L. (2020): The germination of soybeans increases the water-soluble components and could generate innovations in soy-based foods. LWT, 117: 108599.

Cheng C., Zhao X., Yang H., Coldea T.E., Zhao H. (2023): Mechanism of selenite tolerance during barley germination: a combination of tissue selenium metabolism alterations and ascorbate-glutathione cycle modulation. Plant Physiology and Biochemistry, 205: 108189.

Godina R.C., Foroughbakhch R., Mendoza A.B. (2016): Effect of selenium on elemental concentration and antioxidant enzymatic activity of tomato plants. Journal of Agricultural Science, 18: 233–244.

Gupta M., Gupta S. (2017): An overview of selenium uptake, metabolism, and toxicity in plants. Frontiers in Plant Science, 7: 2074.

Hasanuzzaman M., Bhuyan M.H.M.B., Raza A., Hawrylak-Nowak B., Matraszek-Gawron R., Mahmud J.A., Nahar K., Fujita M. (2020): Selenium in plants: boon or bane? Environmental and Experimental Botany, 178: 104170.

Huang Y., Fan B., Lei N., Xiong Y., Liu Y., Tong L., Wang F., Maesen P., Blecker C. (2022): Selenium biofortification of soybean sprouts: effects of selenium enrichment on proteins, protein structure, and functional properties. Frontiers in Nutrition, 9: 849928.

Ikram S., Li Y., Lin C., Yi D., Heng W., Li Q., Tao L., Hongjun Y., Weijie J. (2024): Selenium in plants: a nexus of growth, antioxidants, and phytohormones. Journal of Plant Physiology, 296: 154237.

Jones G.D., Droz B., Greve P., Gottschalk P., Poffet D., McGrath S.P., Seneviratne S.I., Smith P., Winkel L.H.E. (2017): Selenium deficiency risk predicted to increase under future climate change. Proceedings of the National Academy of Sciences, 114: 2848–2853.

Labunskyy V.M., Hatfield D.L., Gladyshev V.N. (2014): Selenoproteins: molecular pathways and physiological roles. Physiological Reviews, 94: 739.

Lei S., Wu Q., Liu Y., Hao M., Liu R., Yu F., Zhang L. (2025): Effects of soaking seeds with selenite on the physiological characteris-

https://doi.org/10.17221/72/2026-PSE

tics and quality of peanut sprouts. Plant, Soil and Environment, 71: 387–397.

Li H.F., McGrath S.P., Zhao F.J. (2008): Selenium uptake, translocation and speciation in wheat supplied with selenate or selenite. New Phytologist, 178: 92–102.

Malik J.A., Kumar S., Thakur P., Sharma S., Kaur N., Kaur R., Pathania D., Bhandhari K., Kaushal N., Singh K., Srivastava A., Nayyar H. (2011): Promotion of growth in mungbean (*Phaseolus aureus* Roxb.) by selenium is associated with stimulation of carbohydrate metabolism. Biological Trace Element Research, 143: 530–539.

Mangiapane E., Pessione A., Pessione E. (2014): Selenium and selenoproteins: an overview on different biological systems. Current Protein and Peptide Science, 15: 598–607.

Qi Z., Ling F., Jia D., Cui J., Zhang Z., Xu C., Yu L., Guan C., Wang Y., Zhang M. (2023): Effects of low nitrogen on seedling growth, photosynthetic characteristics and antioxidant system of rice varieties with different nitrogen efficiencies. Scientific Reports, 13: 19780.

Sun S., Zhang J., Li Y., Xu Y., Yang R., Luo L., Xiang J. (2024): Effects of sodium selenite on accumulations of selenium and GABA, phenolic profiles, and antioxidant activity of foxtail millet during germination. Foods, 13: 3916.

Tan J.A., Zhu W., Wang W., Li R., Hou S., Wang D., Yang L. (2002): Selenium in soil and endemic diseases in China. Science of The Total Environment, 284: 227–235.

Van Hoewyk D. (2013): A tale of two toxicities: malformed selenoproteins and oxidative stress both contribute to selenium stress in plants. Annals of Botany, 112: 965–972.

White L., Castellano S. (2016): The role of selenium in human evolution. In: Hatfield D.L., Schweizer U., Tsuji P.A., Gladyshev V.N. (eds.): Selenium: Its Molecular Biology and Role in Human Health. Cham, Springer, 59–71. ISBN: 978-3-319-41281-8

Yang D., Zhang C., Ma J., Tie Y., Wang S. (2025): Selenium homeostasis and male reproduction. Biochemical and Biophysical Research Communications, 765: 151879.

Zeid I., Gharib Z., Ghazi S., Ahmed E. (2019): Promotive effect of ascorbic acid, gallic acid, selenium and nano-selenium on seed germination, seedling growth and some hydrolytic enzymes activity of cowpea (*Vigna unguiculata*) seedling. Journal of Plant Physiology and Pathology, 7: 1.

Zhang L., Hu B., Deng K., Gao X., Sun G., Zhang Z., Li P., Wang W., Li H., Zhang Z. (2019): NRT1.1B improves selenium concentrations in rice grains by facilitating selenomethinone translocation. Plant Biotechnology Journal, 17: 1058–1068.

Zhang X., Wu G., Wu Y., Tang N., Huang L., Dai D., Yuan X., Xue C., Chen X. (2024): Diversity analysis and comprehensive evaluation of 101 soybean (*Glycine max* L.) germplasms based on sprout quality characteristics. Foods, 13: 3524.

Zhou Y., Nie K., Geng L., Wang Y., Li L., Cheng H. (2024): Selenium's role in plant secondary metabolism: regulation and mechanistic insights. Agronomy, 15: 54.

Received: February 8, 2026
Accepted: April 17, 2026
Published online: May 21, 2026